OFFICE OF NAVAL RESEARCH

Contract N-00014-91-J-1627

R & T Code 413j010---04

TECHNICAL REPORT NO. 1

Discrimination in Resolving Systems:

Ephedrine-Mandelic Acid

by

Edward J. Valente[1], Jeffrey D. Zubkowski[1] and Drake S. Eggleston[2]

[1]Jackson State University
Department of Chemistry
Jackson, MS 39217

[2]Department of Physical & Structural Chemistry
Smith Kline & Beecham Pharmaceuticals
King of Prussia, PA 19406

7 February 1992

Discrimination in Resolving Systems: Ephedrine-Mandelic Acid

by

Edward J. Valente[1], Jeffrey D. Zubkowski[1] and Drake S. Eggleston[2]

[1]Jackson State University
Department of Chemistry
Jackson, MS 39217

[2]Department of Physical & Structural Chemistry
Smith Kline & Beecham Pharmaceuticals
King of Prussia, PA 19406

Abstract

Resolution of mandelic acid with (1R,2S)-(-)-ephedrine in water and ethanol produces intermediate diastereomeric salts with greatly disparate solubilities and melting points. Single crystal x-ray analysis of the less (L) and more (M) soluble (-)-ephedrinium mandelates (I, II) shows crystal structures which are isosteric, each crystallizing in the monoclinic system, space group C2. Protonated ephedrines occupy the same relative positions in the L- and M-salts, and mandelates are in the same general locations. Hydrogen bonds link alternating protonated ephedrine nitrogens and mandelate carboxylate oxygens in each salt forming columns of ions. The helical H-bonded chain winds down the crystallographic two-fold screw axis. Additional H bonds form between two-fold related mandelates in the L-salt. Mixed crystals, containing both mandelate isomers, (2R)- and (2S)-mandelates, are obtained from the resolving system partly depleted of the L-salt. A specimen with nearly equal amounts of the mandelates (III) is also isosteric with the commensurate structures.

I (294K), L-salt: a = 18.160(7), b = 6.538(2), c = 13.898(4)Å^3, ß = 92.02(3)° , V=1649.1(9)Å^3; **IIa** (294K), M-salt: a = 17.978(11), b = 7.164(4), c = 13.574(6)Å^3, ß = 96.41(4)°, V = 1737.3(16) Å^3; **IIb** (223K), M-salt: a = 17.805(8), b = 7.115(2), c = 13.50(5)Å^3, ß = 96.89(3), V = 1704.0(15)Å^3; **III** (294K), mixed-salt: a = 18.184(22), b = 6.792(7), c = 13.808(19)Å^3, ß = 93.74(10)°, V = 1701.7(35)Å^3.

INTRODUCTION

Classical resolution of racemic acids involves the formation of intermediate diastereomeric salts with a homochiral complementary base (resolving agent). Among the classical methods of discrimination, the salts are commonly separated on the basis of disparate solublilities. The (partly) resolved acid is liberated by subsequent chemical treatment. Hundreds of resolutions have been successfully accomplished by these and analogous methods using a collection of naturally occurring homochiral resolving agents[1,2].

For resolution of salts by differential solubility, a chemist takes advantage of the consequences arising from differences in cohesion exhibited by the diastereomeric phases. It is tempting to expect such differences chiefly or rationally to result from the number and strength of pairwise ionic aggregates. Crystallization of diastereomeric salts involves a balance between ion-solvent and ion-lattice interactions during growth. Differences include the number, type and strength of interactions, the presence or lack of cocrystalyzed solvent, and the packing arrangement and crystal system. For example, solubilities of diastereomeric α-phenylethylammonium hydratropates in ethanol differ by less than a factor of two at ambient temperature, with the less soluble (L) salt having the higher fusion point.[3] Brianso[4] has compared the structures of these diastereomers and found that the dominant interactions in the crystals occur through alternating H-bonding between ammonium and

carboxylate moieties arranged helically along a crystallographic 2_1 axis. Columns of ions are tightly held thus, while weaker van der Waals forces govern the attractions between the columns. In each structure, the number of H-bonds is the same, but their length is slightly less in the L-salt, and the helical repeat distance (corresponding with a cell translation) is also shorter. Since the structures are closely related and the discriminating features are rather subtle, a satisfying qualitative correlation with the observed physical properties of the diastereomers emerges. Crystallography therefore is a useful tool for examining the structural basis underlying practical resolving systems.

In the present study, we continue an examination of the ephedrine-mandelic acid system. Jaworski & Hartung[5] found that ephedrinium mandelate salts had greatly different solubilities and fusion temperatures. The less soluble (L) salt, dissolves to the extent of 6.0g in 100g of water. In contrast, 77.5g of the more soluble (M) dissolves in 100g water at 298K. Relative stabilities of the salts toward dissolution in highly polar media correlate with their fusion temperatures; the L-salt fuses at 443K, the M-salt broadly through 351-362K. The ephedrine-mandelic acid system is remarkable among such compounds in that its salts have such markedly different physical properties.

In part, the crystallography underlying these disparities was reported by Zingg *et al.*[6] The L-salt described had a fusion point consistent with the phases obtained from ethanol[5,7],

water[8], or isopropanol[9]. However, the M-salt was recrystallized from benzene, and had a melting about 384K, significantly larger than the 351-362K obtained for this phase from ethanol and ether-ethanol mixtures[5]. The structures of the diastereomers were found to form columns of H-bonded ions, to be devoid of solvent, and in different crystal systems. Crucially, the M-salt was found to have fewer interionic interactions than the E-salt, correlating with the differences between their fusion temperatures, heats of fusion and solution.

Our preliminary studies of the ephedrine-mandelic acid salts crystallized from 95% ethanol suggested that the M-salt might show polymorphism. The M-salt isolated by Zingg et al.[6] appeared to be unlike that obtained by Jaworski & Hartung[5]. Since the phases obtained from the latter's resolution of mandelic acid with ephedrine in polar media may display even more disparate properties, a reexamination of the salts was indicated. In this study, we examine the phases of ephedrinium mandelate formed from ethanol and/or water solutions equimolar in racemic mandelic acid and (-)-(1R,2S)-ephedrine.

EXPERIMENTAL

Reagents and high purity solvents were used as obtained from Aldrich Chemical Co. Optical rotations were measured with a Perkin-Elmer 141 polarimeter using a 1.00dm tube. Heats of fusion were determined on an DuPont 9900 Differential Scanning Calorimeter.

Resolution of Mandelic Acid. Combine equimolar quantities of (-)-(1R,2S)-ephedrine and (±)-mandelic acid at room temperature in 95% ethanol. Colorless prisms of the L-salt begin to separate in a few minutes. After 5h, filter the L-salt and recrystallize from a minimum of warm water; the large colorless prisms have mp 443K, $[\alpha]_D$ -75.6(1)°, c 2.4 in H_2O at 295K, ΔH_{fus} 11.8kcal·mol^{-1} (lit.[5] mp 443K, $[\alpha]_D$ -70.6°, c 2.4 in H_2O at 300K and lit.[6] mp 439-440K, $[\alpha]_D$ -78.9° at 298K, ΔH_{fus} 12.3(4)kcal·mol^{-1}). Concentrate the filtrate by evaporation; some additional colorless crystals separate with broad mp's less than 433K. From the resulting viscous mixture, the M-salt forms a mass of colorless crystals eventually; dry these a vacuum to produce a sample with broad mp about 353K. Recrystallize the M-salt from 9:1 ethyl ethanote:ethoxyethane producing smaller colorless prisms, mp ≈ 370K (capillary), $[\alpha]_D$ +22.7°, c 2.8 in H_2O at 294K; or from 9:1 ethyl ethanoate:ethanol producing somewhat larger colorless elongated prisms, mp 367-372K (capillary) but only 348K (DSC), $[\alpha]_D$ +28.9(1.8)°, c 0.5 in H_2O at 297K, ΔH_{fus} 2.97kcal·mol^{-1} (lit.[5] mp 351-364K, $[\alpha]_D$ +21.3°, c 2.8 in H_2O at 299K; contrast with lit.[6] ΔH_{fus} 6.5(1) kcal·mol^{-1}). Specimens of the M-salt from 95% ethanol, ethyl ethanoate:ethoxyethane or ethyl ethanoate: ethanol have the same space group and cell constants (see Abstract).

Absolute stereochemistry of the mandelate ions was established relative to the known 1R,2S configuration of (-)-ephedrine used in the resolution. By Walden's rule[11], the L-salt is (-)-

(1R,2S)-ephedrinium (-)-(2R)-mandelate, and the M-salt (-)-(1R,2S)-ephedrinium (+)-(2R)-mandelate. These were subsequently confirmed by crystallography.

Crystallography. Crystals studied were those from solutions in polar solvents. Preliminary Weissenberg and precession photography on a crystal of the L-salt revealed patterns consistent with a centered monoclinic lattice and probably space group C2 (#5). Crystalline specimens of the L- (I), M- (IIa) and the mixed salts (III) were chosen for data collection on a Siemens R3M/V automated diffractometer using Mo Kα radiation ($\lambda\bar{\alpha}$ 0.71073Å) at 294K: I, 0.65 x 0.55 x 0.25 mm^3; IIa, 0.54 x 0.28 x 0.5 mm^3; III, 0.6 x 0.4 x 0.3 mm^3. A second crystal of the M-salt, IIb, 0.4 x 0.25 x 0.2 mm^3, was used for a lower temperature (223K) determination using Cu Kα radiation ($\lambda\bar{\alpha}$ 1.5418) and a CAD-4 automated diffractometer. Twenty accurately centered reflections with $32^\circ < \theta < 60^\circ$ were used to establish cell constants. Common to all three crystals: formula $[C_{10}H_{16}NO]^+$ $[C_8H_7O_3]^-$, M_r = 317.40, monoclinic, space group C2 (#5), Z = 4, F(000) = 680, T = 294K. Other information for I, V = 1649.1(9)$Å^3$, D_x = 1.278 Mg/m^3, μ = 0.084 cm^{-1}; for IIa, V = 1731.3(15)$Å^3$, D_x = 1.218 Mg/m^3, μ = 0.080 cm^{-1}; for IIb, V = 1704.0(15)$Å^3$, D_x = 1.237 Mg/m^3, μ = 0.814 cm^{-1}; for III, V = 1702(4)$Å^3$, D_x = 1.239 Mg/m^3, μ = 0.081 cm^{-1}. Intensity data were measured from $2\theta = 3.5^\circ$ to 74° (I), to 58° (IIa), to 55° (III), and from 2° to 112° (IIb); for I, h: -30 to 30, k: 0-11, l: 0-23; for IIa, h: -24 to 24, k: 0-9, l: 0-18; for IIb, h: 0 to 23, k: 0-9, l:-17 to 17; for III, h: -23 to 23, k: 0-8, l: 0-17. The

data (4691 for I, 2587 for IIa, 2294 for IIb, and 3209 for III) were corrected for Lorentz and polarization effects. Three intensities each were monitored periodically over the course of the data collections. From these, small linear decay corrections were applied to the raw data collected between the monitored intensitites. Then, symmetry equivalent data were averaged, leaving 4508 (I), 2500 (IIa), 2222 (IIb), and 2130 (III) unique intensities.

The structure of the L-salt (I) was determined using direct methods (SHELXTL[13]) and refined by full-matrix least-squares methods. Non-H-atom positions were refined with their isotropic temperature factors minimizing $\Sigma w(|F_o|-|F_c|)^2$, with $w = 1$; then with their anisotropic temperature factors and with $w = (\sigma_F^2 + f \cdot F^2)^{-1}$ where $f = 9.0 \times 10^{-4}$. The y-coordinate of the ephedrine nitrogen was fixed at 1/15; similarly in IIa,b and III. H-atom positions were located in difference Fourier maps but placed at calculated positions adjacent to their attached atoms. They were assigned U's of 0.080Å^2, and their positions adjusted accordingly during refinement of the non-H atoms. Extinction and absorption corrections were not applied. Scattering factors were taken from International Tables for X-ray Crystallography[12]. Programs employed were those of the SHELXTL PLUS and CAD4-SDP[13] systems. Absolute configuration of the mandelate ion corroborates the chemical inferences from the known 1R,2S assignment of (-)-ephedrine; the L-salt contains the (2R)-mandelate. Refinement converged at R = 0.073, wR = 0.084 for 3796 reflections with $I > 3\sigma_I$ and 208 variables. Goodness-of-fit was 1.80 and a final

difference Fourier map showed no features larger than +0.40, $-0.26 e\text{Å}^{-3}$. Atom positions are given in Table I.

Noting the common space group C2 and the similarity in the lattice constants of the three crystals, models for the structures of IIa,b and III were tested by computing difference Fourier maps based on the coordinates for the non-H atoms in the ephedrinium ion from I. All non-H atoms of the mandelate ion in IIa,b were located initially in this way. In the position expected for the mandelate ion in III, maps showed two essentially distinct mandelates of opposite hand occupying the site. These were further modelled by identifying the non-H atoms of each ion and refining associated occupancy factors with their sum constrained to unity.

Least-squares refinements of the models for IIa,b and III proceeded as for I with H's in calculated positions and using f = 9.5×10^{-4} (IIa, III) and 6.4×10^{-3} (IIb) in the weighting expression. Phenyl rings atoms of each mandelate in III were close enough in the model to require treatment as rigid groups with isotropic temperature factors at first and then with anisotropic temperature factors for each carbon. The model for III was given additional stability by refining the isomeric phenyl ring atoms and temperature factors in alternate cycles and damping the applied shifts in the final stages. The models converged with final R factors of 0.093 (IIa), 0.075 (IIb), 0.085 (III), weighted R factors of 0.108 (IIa), 0.096 (IIb) 0.096 (III). Models were refined against 905 (IIa), 1690 (III) data with $I \geq 3\sigma_I$ and 207 (II), 196 (III) variables, and 1252 (IIb)

data with $I \geq 2\sigma_I$ and 207 (IIb) variables. Goodness-of-fit was 2.33 (IIa), 1.58 (IIb), 2.11 (III) and final difference Fourier maps showed no features larger than +0.38, -0.30eÅ^{-3} (IIa), +0.34, -0.28eÅ^{-3} (IIb), +0.25, -0.29eÅ^{-3} (III). The M-salts (IIa,b) contain the 2S-mandelate ion, and the final occupancy factor for the 2S-mandelate contribution in III was 0.440(2).

Atom positions and equivalent isotropic temperature factors are given in Tables I - IV. Hydrogen bonding information is presented in Table V; positions of the anions and cations in the similar cells are compared in Table VI. Bond lengths and angles for all the structures are set out in Tables VII and VIII. Thermal ellipsoid plots of the ions in each structure are given in Figures 1 - 4, and unit cell drawings are given in Figures 5 and 6. Tables of anisotropic temperature factors, calculated H-atom positions, and the observed and calculated structure factors are available from the authors.

Results and Discussion

Considering the relatively large differences in the melting temperatures and solubilities of the diastereomeric (-)-ephedrinium mandelates found by Jaworski & Hartung[5], one might have expected differences in solvation or crystal structure. Both the L- (I) and M- (II) salts from ethanol, however, are found in the same space group with similar cell constants. Each salt is unsolvated, hydrogen bonding between ions furnishes the principal cohesive interactions, and their structures are

isosteric. The concept of isostery implies a broad view of crystal structural similarity in which a kind of molecular replacement or "molecular isomorphism" occurs. Ephedrinium and mandelate ions occupy about the same general locations in both I and II. They are distinguished rather on the basis of the number and kind of interionic interactions formed. As summarized in Table V, the L-salt (I) forms six interionic interactions and the M-salt (II) forms three. Since the processes of melting and dissolution depend on cohesion in the crystal, and the crystal structures are isosteric, the L-salt is understandably the higher melting diastereomer. Fewer interactions in the M-salt contribute to a diminished packing efficiency resulting in a cell volume some 4.9% higher than for the L-salt.

Isostery between the structures of the diastereomeric ephedrinium mandelates is further emphasized by the existence of a mixed salt, phase III. In the crystal of this substance chosen for study, 44% of the mandelates are the (2S)-isomer, 56% are the (2R)-isomer. The cell volume in III is intermediate between that of the pure phases and its crystal structure is similar then to either relative I or II. Ephedrine moieties are found essentially in the same relative positions and conformations as in the pure diastereomers. Mandelates of opposite hands appear superimposed, and occupy positions with general orientations similar to those observed in the L- and M-salt phases (Table VI).

Unit cell drawings projected along the **b** (screw) axis for I and II, Figures 5 and 6, respectively show that anions and cations do not form isolated H-bonded pairs. Rather, in each

structure, infinite chains of H-bonds coil along the crystallographic two-fold screw axes, linking ephedrinium and mandelate ions alternately through the protonated secondary ammonium and carboxylate groups (Table V). The L-salt (I) is the (-)-ephedrinium (-)-mandelate. Its structure is identical to and enantiomeric with that of the (+)-ephedrinium (+)-mandelate previously described[6]. A brief discussion is included here as a basis for comparison with the other diastereomer II and the mixed salt III.

The principal cohesive associations in the L-salt (I) are the distinctive H-bonds between ions which form helical columns. Of the three donor-acceptor interactions found in the column, two occur through a bifurcated H-bond, $N\text{-}H_a:::[O(3),O(4)]$ with an overall $R_1^2(4)$ pattern[14] [a 4-ring with one donor and two acceptor atoms]. The other is a single interaction $O(4)\cdots H_bN'$. The infinite chain involves a repeat $C_2^1(4)$ [four atom chain with one acceptor and two donor groups] pattern through the bifurcated H-bonded rings along the screw axis, and each occurs twice within a cell. Also within the column, ephedrines and mandelates each donate an hydroxyl H-bond to separate carboxylate oxygens. Columns are tied together through mandelate H-bonds which link pairs of anions around the neighboring two-fold axes, and which have an $R_2^2(10)$ [10-ring with two donor and two acceptor atoms] pattern. In all, each mandelate ion in the L-salt forms six H-bonded interion associations, one as a donor and five as an acceptor (Figure 5). Ephedrinium ions form four donor associations with three different neighboring mandelate ions and none

with other cations.

While anions and cations are potentially able to form intraionic O-H···O or N-H···O hydrogen bonds, none are evident. In the cations, both ammonium hydrogens engage in interionic H-bonding, and the O-C-C-N^+ torsion angle [-55.1(2)°] is far from a planar arrangement. In the anions, mandelate hydroxyl hydrogens engage in H-bonding with neighboring two-fold related mandelates in the 10-ring described above. The mandelate O-C-C-O^- torsion angle is only 11.9°, but this serves the H-bonding across the two-fold axes between pairs of mandelates (Figure 5).

Alternating anions and cations in the M-salt (II, (-)-ephedrine (+)-mandelate) form a related but distinct set of helical H-bonds along the screw axes compared to those in I. Mandelate carboxylate group adopts a different orientation to that found in the L-salt (I). As a result, direct rather than bifurcated H-bonds form (Table V and Figure 6) with one carboxylate oxygen through the repeating $C_2^1(4)$ pattern. As in I, the other carboxylate oxygen accepts another H-bond from a third neighboring cation through the ephedrine hydroxyl. However, no close intermandelate associations occur across the two-fold axes nor are any intraion H-bonds are evident in II also. The O-C-C-O^- torsion angle is only 8.5° but the hydroxyl oxygen displays quite large vibrational motion (at 294K and at 223K) which prevents location of its hydrogen and suggests that no H-bond is formed. In all, mandelate ion in II forms acceptor H-bonded interion associations with three neighboring ephedrines

(Figure 6). Each of these is shorter than the corresponding interactions in I (Table V). Nevertheless, atoms of the mandelate hydroxyl and phenyl groups in II have significantly larger thermal vibrations than these groups in the L-salt (I).

As mentioned above, vibrational amplitudes at 294K for the atoms in the M-salt (IIa) are quite large. A lower temperature determination (IIb) was performed to test whether these thermal vibrations obscured some disorder or contamination by a small amount of (2R)-mandelate. Vibrations of all M-salt non-H atoms diminish by about 40% on cooling from 294K to 223K (compare temperature factors in Table II and Table III); no signature evident of disorder or partial anion replacement could be seen.

The mixed crystal, III, is a phase in which (2R)- and (2S)-mandelates are more or less randomly distributed in the structure, or contained in (many?) distinct crystalline domains. Either situation could give rise to modest lattice distortions resulting in somewhat less accurately determined cell constants and an intermediate cell volume compared to the commensurate phases. Ephedrinium ions in III are ordered and have conformations like those in the L- and M-salts (Table VI). Mandelates are found in III to occupy anionic sites in almost equal proportions and in such an orientation that their hydroxyl groups [O(2) and O(2B)] are at nearly the same position. Carboxylate planes are oriented about 90° with respect to each other. Contact distances between likely H-bond donors and acceptors suggest that all of the interionic interactions seen in I and II are present, plus possibly one additional interaction between unlike enantio-

meric mandelates (see Table V).

To perceive the difference between the commensurate and the mixed mandelate structures, recall the H-bonded pairing of mandelates about two-fold axes in the L-salt and the lack of such interion interactions in the M-salt. In the mixed crystal, mandelate pairs may exist in three distinct groupings: (2R)-mandelate next to (2R)-mandelate, (2S)-mandelate next to (2S)-mandelate, and (2R)-mandelate next to (2S)-mandelate. In the first case, intermandelate H-bonds form and the other five mandelate-ephedrine interactions are present and similar to those in the L-salt. Correspondingly, in the second case, no intermandelate H-bonds form and the other three mandelate-ephedrine interactions are present and similar to those in the M-salt.

When unlike mandelate enantiomers are adjacent, as in the third case, the two-fold axis necessarily fails and a pseudoracemate relationship exists between the mandelates. This may occur at random locations through the crystal or between domains depending on the nature of the mixed crystal. The conformations of the mandelates are, however, not related by centrosymmetry. Instead the mandelate conformations allow (2R)-mandelate carboxylates to accept H-bonds from adjacent (2S)-mandelate hydroxyl while the complementary H-bond cannot form. Mixed crystals show two mandelate orientations, instead of three. In one case, where (2R)-isomers are next to (2R)- or (2S)-mandelates, five or six of the six interionic interactions available occur, respectively, compared with the L-salt. Five of six is enough appar-

ently to give the same mandelate conformation as when all six occur. The other orientation develops around (2S)-mandelates which form the same three interactions as in the M-salt plus one more if it is adjacent to a (2R)-isomer. An additional H-bond forms apparently without a significant conformational change of the mandelate. Mandelate conformations in the mixed crystal differ enough from those in the pure phases to suggest that the two kinds of mandelate ions are likely distributed throughout the crystal rather than locked in domains containing one hand or the other. The orientation of either mandelate enantiomer is larely determined by the interactions with the ephedrine cations. As seen in each of the commensurate phases, these consist of similar infinite H-bonded chains along the screw axes. Where opposite mandelate isomers are adjacent, addition or deletion of one intermandelate interaction may therefore plausibly occur without strongly affecting the other's orientation.

Comparison of More Soluble Salt Phases. The M-ephedrinium mandelate from resolution in ethanol crystallizes in the monoclinic system. Zingg[6] has described the structure of an orthorhombic M-salt phase obtained from (+)-ephedrine and (-)-mandelic acid (or from their respective enantiomers) and recrystallized from benzene. Both have infinite chains of H-bonds linking protonated ephedrines with one of the mandelate carboxyl oxygens along a screw axis, and the repeating H-bonding pattern $C_2^2(4)$.

These phases chiefly differ in relative position of the H-bonded chains and in the number of other interion associations. Perpendicular to the H-bonded screw axis, the orthorhombic phase

shows a distorted hexagonal arrangement of H-bonded columns around each with two at 8.9Å and four at 16.5Å distant. Columns are arranged rectilinearly in projection down the unique (screw) axis in the monoclinic phase with two at 9.0Å, 13.6Å each. Two chains penetrate through the cell of each type and the chain repeat distances and cell area in cross-section are virtually the same. In the orthorhombic phase, hydroxyls on both ephedrine and mandelate ions are additionally H-bonded to neighboring mandelate carboxyl oxygens. In the monoclinic, an ephedrine hydroxyl forms an H-bond with a neighboring mandelate carboxyl oxygen, but the ephedrine hydroxyl does not form an interionic H-bond. In all, therefore, four H-bonds contribute to the cohesion of the orthorhombic M-salt structure compared to three H-bonds in the monoclinic phase. This accords with the greater fusion point for the orthorhombic phase (384K) compared to the monoclinic (below 372K).

Observations on Molecular Discrimination. The ephedrinium mandelates are members of the series of "organoammonium carboxylates". Brisano[4] pointed out the importance of the H-bonded helical arrangement of alternating cations and anions in the crystal structures of members of this series. Table IX provides a summary of some crystal data and physical properties for compounds in this class for which the structures of both diastereomeric salts are known. In general, the L-salts are characterized by a shorter axial repeat distance along the helical H-bonded chain than for the M-salts. This results usually in more compact structures (lower cell volumes, greater densities, higher

fusion temperatures). A possible exception is the pseudoephedrinium mandelate diastereomers between which there is little difference in melting point, and the salt having the greater fusion enthalpy (presumably also the L-salt) actually has the larger cell volume.

For the group of organoammonium carboxylates, similar infinite H-bonded helical chains wrap down two-fold screw axes and make up the primary associations between ions. Two H-bonds, between ammonium ion and one or both of the carboxylate oxygens (whether one is bifurcated or not), comprise the $C_2^1(4)$ and $C_2^2(6)$ motifs in all the related structures summarized in Table IX. Where the number of H-bonds along the helical axis is the same for each diasteromeric salt, the fusion temperatures are not much different. In the ephedrinium mandelates, additional H-bonds form in the L-salts between columns of ions. Even though the cells are similar in dimensions and the ions are found in the same general locations within them, these added interactions contribute significantly to the stability of the L-salt lattice compared to the M-salt. They give rise to a large and discriminating cohesive difference between the diastereomeric salts.

Acknowledgements

We are grateful to the Office of Naval Research, DURIP Grant No. 88450-0340, and the National Institutes of Health, AREA Grant No. GM42198 for diffractometry equipment in Central Mississippi. Additionally, we thank Dr. Jeanette Krause, Mr. Jimmy L. Boyd and Mr. Donald Thomas for their experimental assistance.

Literature Cited

1. Wilen, S. H. "Tables of Resolving Agents and Optical Resolutions", c. 1972, University of Notre Dame Press, Notre Dame, Indiana.

2. Jacques, J., Collet, A. and Wilen, S. H., "Enantiomers, Racemates, and Resolutions", c. 1981, John Wiley & Sons, New York.

3. Leclercq, M. & Jacques, J. Study of Optical Antipode Mixtures. X. Separation of Complex Diastereomeric Salts by Isomorphism. Bulletin of the Chemical Society, France (Part 2) 1975: 2052-2056.

4. Brianso P. A Crystallographic Explanation of the Separation or Cocrystallization of the Diastereomers of 1-Phenylethylammonium 2-Substituted Phenylethanoates. Acta Crystallographica B37: 618-620, 1981.

5. Jaworski, C. & Hartung, W. H. Amino alcohols. XII. Optical isomers in the ephedrine series of compounds. Journal of Organic Chemistry 8: 564-571, 1943.

6. Zingg, S. P., Arnett, E. M, McPhail, A. T., Bothner-By, A. A., Gilkerson, W. R. Chiral Discrimination in the Structures and Energetics of Association of Stereoisomeric Salts of Mandelic Acid with α-Phenethylamine, Ephedrine, and Pseudoephedrine. Journal of the American Chemical Society 110:1565-1580, 1988.

7. Manske, R., Johnson, T. Synthesis of Ephedrine and Structurally Similar Compounds. II. The Synthesis of Some Ephedrine Homologs and the Resolution of Ephedrine. Journal of the American Chemical Society 51:1906-1909, 1929.

8. Rogers, R. Resolution of dl-Mandelic Acid with (-)-Ephedrine. Journal of the Chemical Society, 1544-1547, 1935.

9. Skita, A., Keil, F., Meiner, H. Kernhydrierte Optisch Activ Ephedrine. Chemische Berichte 66:974-984, 1933.

10. Smith, E., Worrell, L. F., Sinsheimer, J. E. The Amperometric Determination of Amines. Analytical Chemistry 35:58-63, 1963.

11. Walden, P. Zeitschrift fur Physicalische Chemie 15: 196-200, 1894.

12. International Tables for X-ray Crystallography Volume IV, Birmingham: Kynoch Press (present distributor: Klewer Academic Publishers, Dordrecht, The Netherlands) 1974.

13. SHELXTL PLUS (System of crystallographic programs) Siemens Analytical X-ray Instruments, Incorporated, Madison, WI. 1990; and SDP (System of crystallographic programs) Enraf-Nonius Company, Bohemia, NY. 1990.

14. Etter, M. C. Encoding and Decoding Hydrogen-Bond Patterns of Organic compounds. Accounts of Chemical Research 23:1120-1126, 1990.

15. Brianso, P. Atomic and molecular structures of the diastereomeric α-phenylethylammonium α-phenylacetates. Acta Crystallographica B32:3040-3045, 1976.

16. Brianso, P. Atomic and Molecular Structure of n (-)-1-phenylethylammonium (+)-2-phenylbutanoate. Acta Crystallographica B34:679-680, 1978.

17. Brianso, P. Atomic and Molecular Structure of p 1-phenylethylammonium 2-phenylbutanoate. Acta Crystallographica B37:740-741, 1981.

18. Brianso, P., Leclercq, M., Jacques, J. 1-Phenylethylammonium mandelate. Acta Crystallographica B35:2751-2753.

Figure 1. Thermal ellipsoid plot of the atoms in the L-salt (I) showing heteroatom numbering and enclosing 50% probability density.

Figure 2. Plot of the atoms in the M-salt (IIa) at 294K.

Figure 3. Plot of the atoms in the M-salt (IIb) at 223K.

Figure 4. Plot of the atoms in the mixed salt (III). (2S)-Mandelate shown with open bonds (IIIA); (2R)-mandelate with filled bonds (IIIB).

Figure 5. Plot of the unit cell of the L-salt (I) viewed approximately along the **b** axis. Hydrogens omitted except those on nitrogen and oxygen; dashed lines indicate H-bonds.

Figure 6. Plot of the unit cell of the M-salt (II) viewed approximately along the **b** axis. Hydrogens omitted except those on nitrogen and oxygen; dashed lines indicate H-bonds.

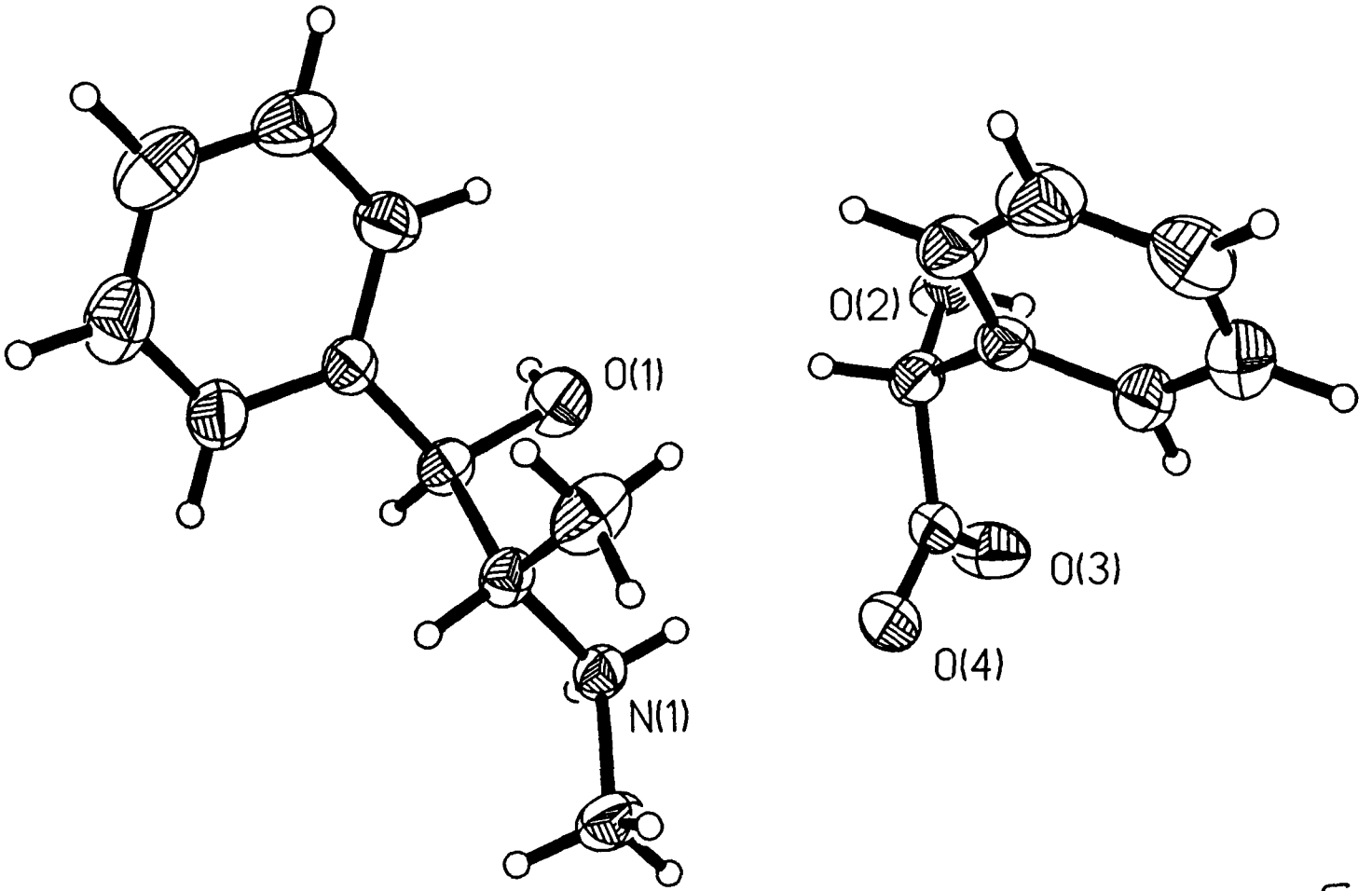

Fig. 1

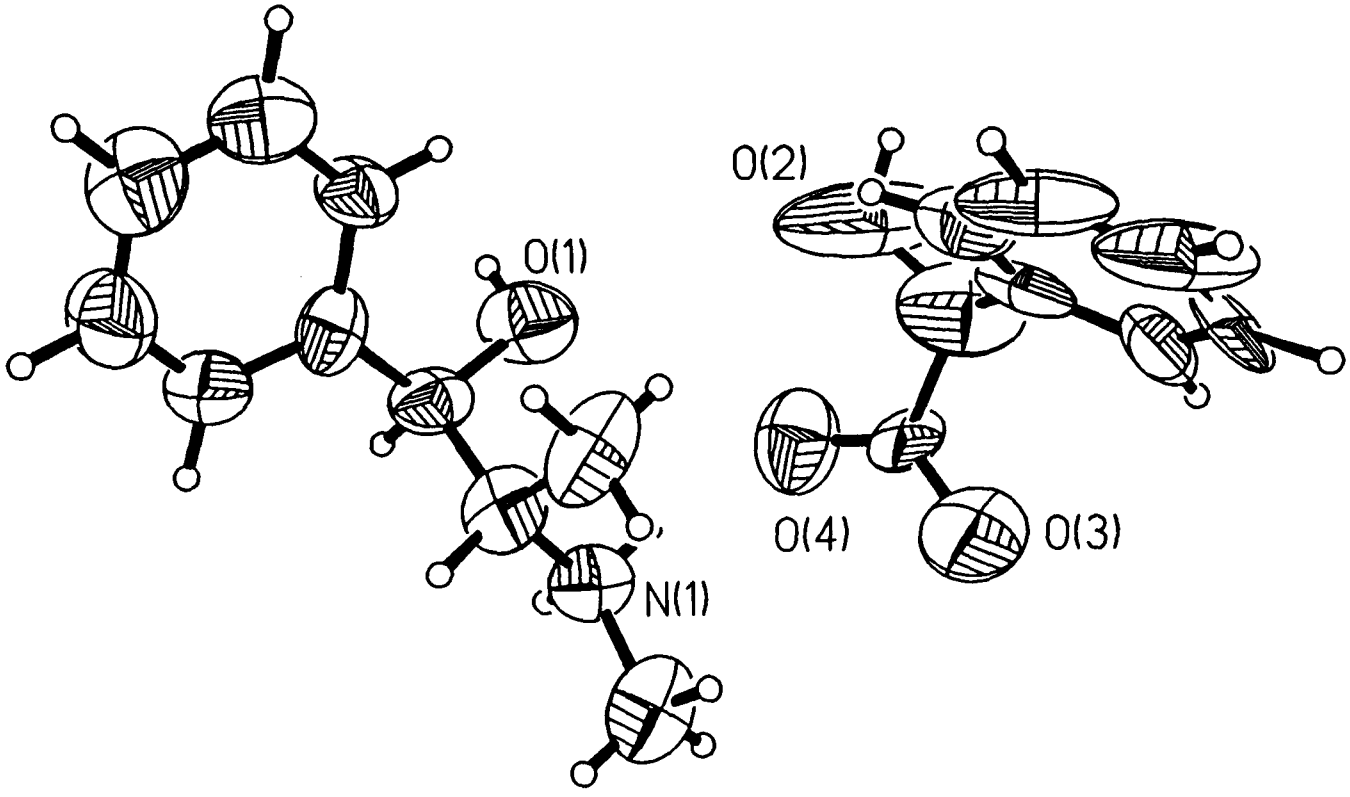

Fig. 2

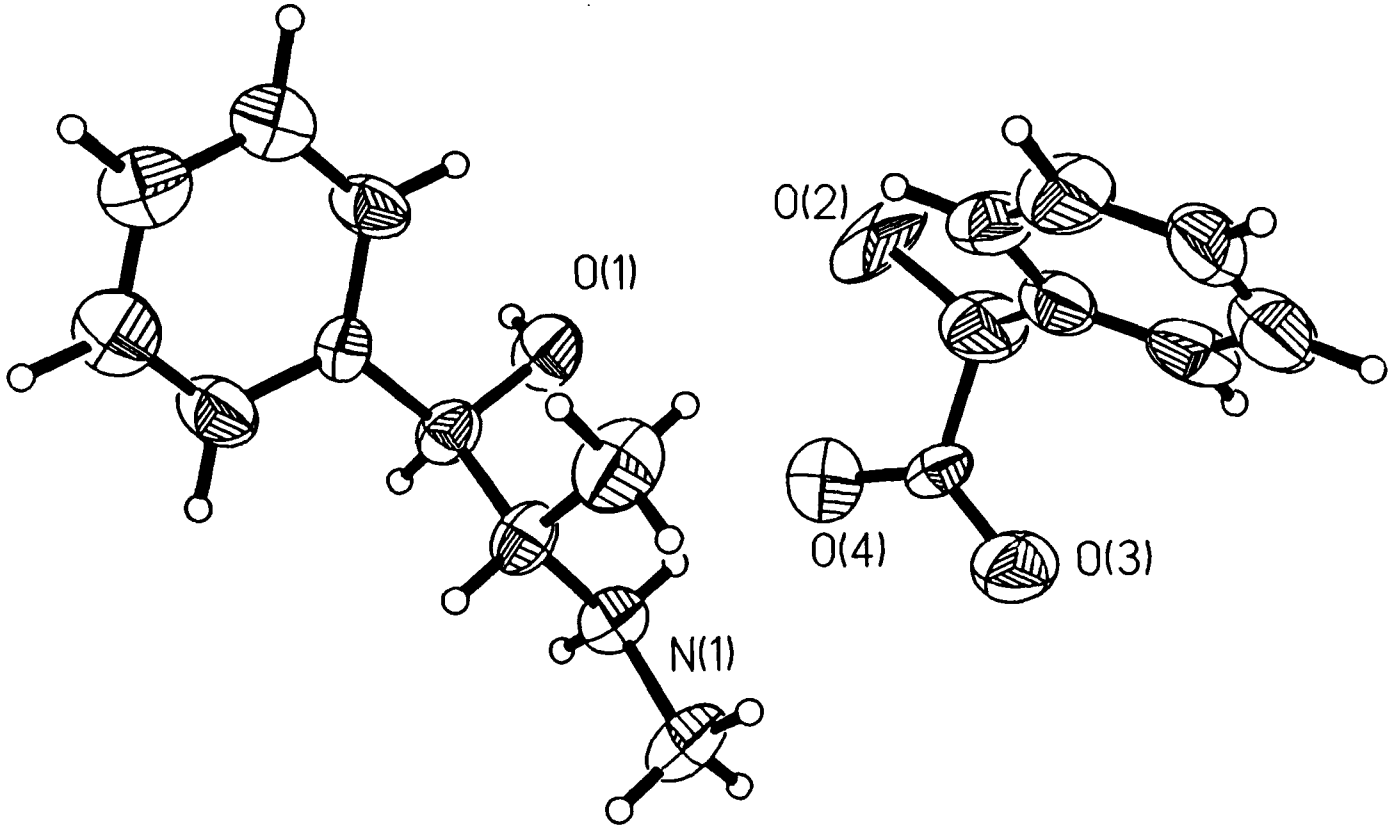

Fig. 3.

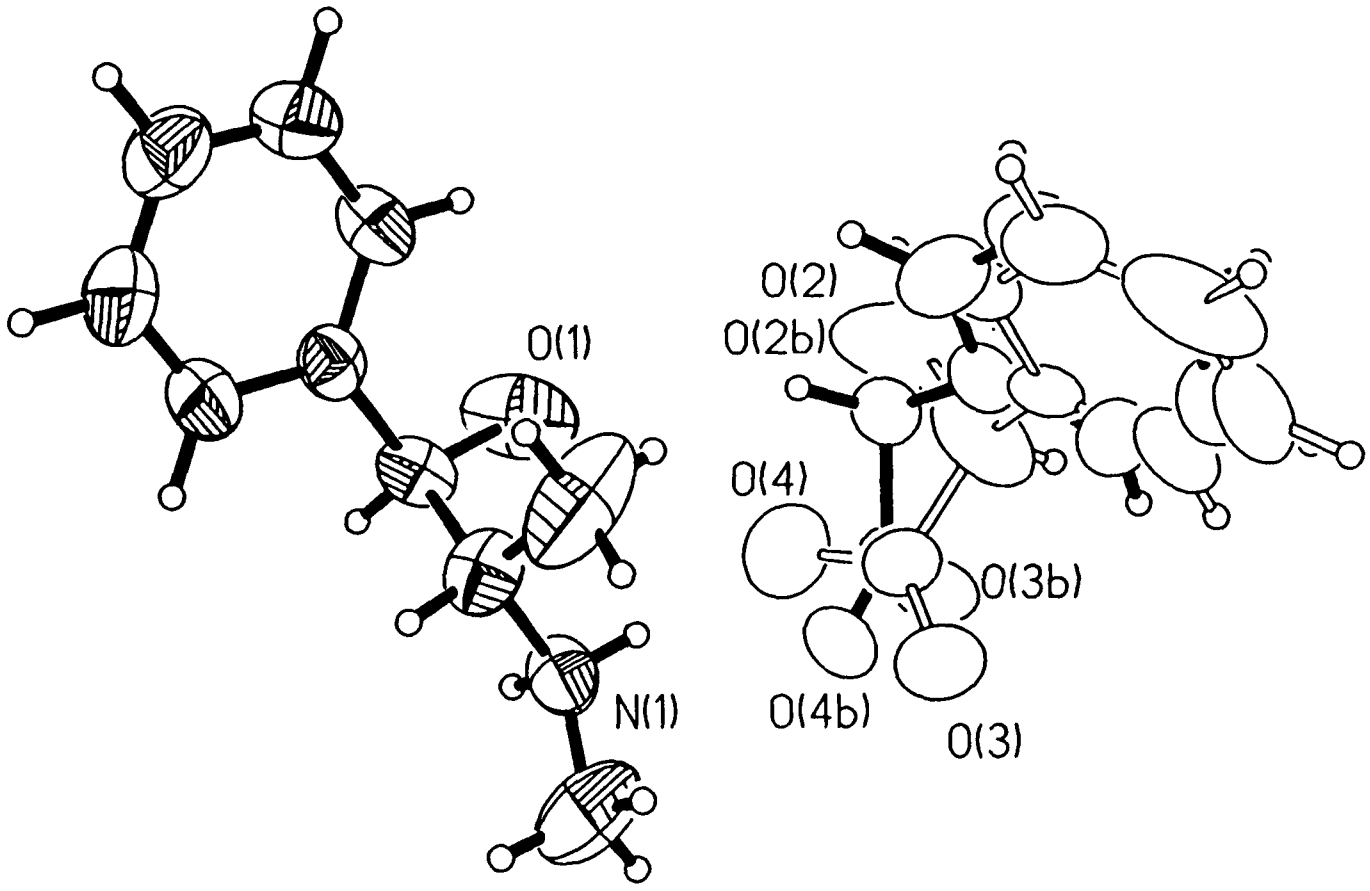

Fig. 4.

Fig. 5.

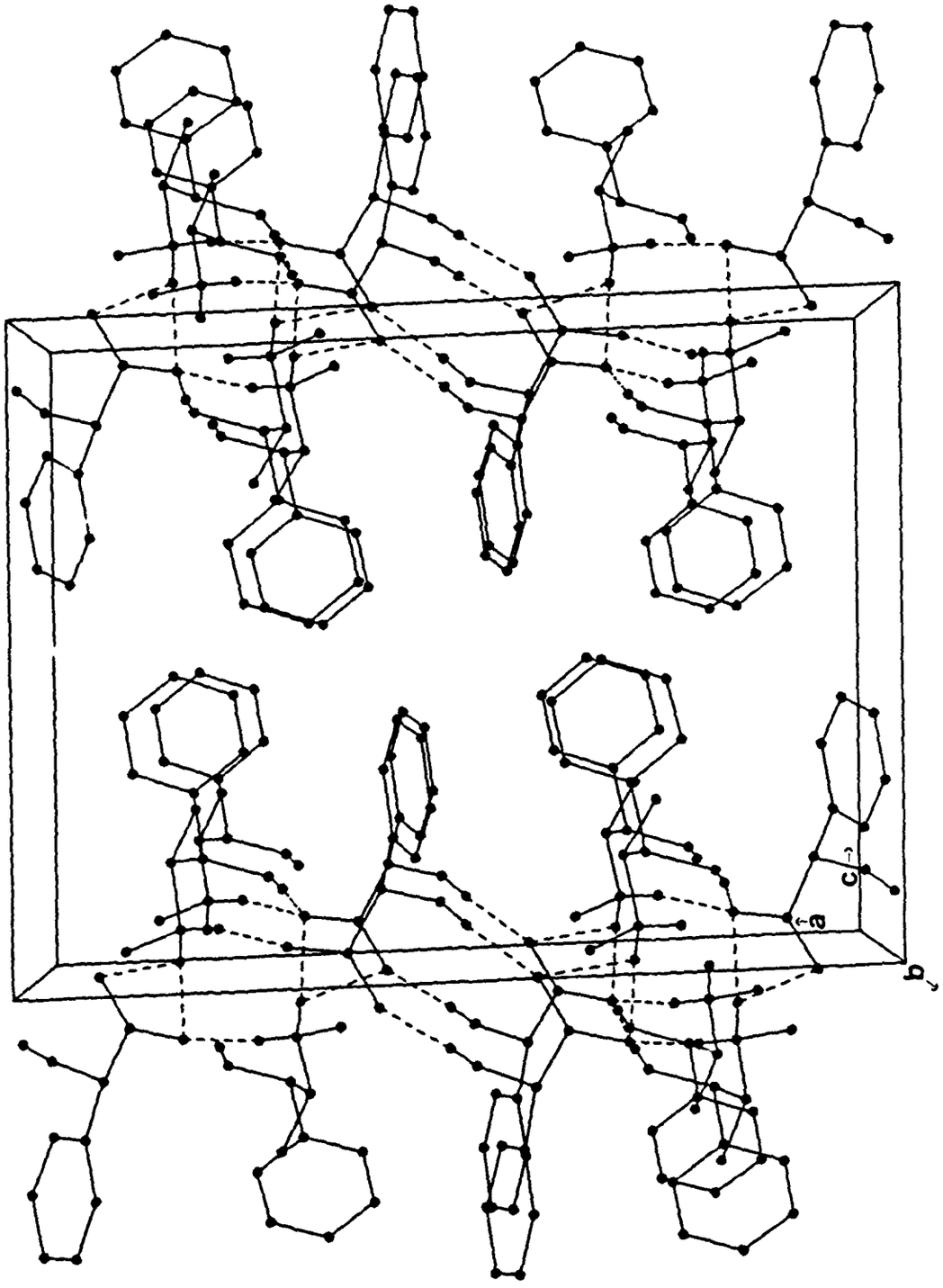

Fig. 6.

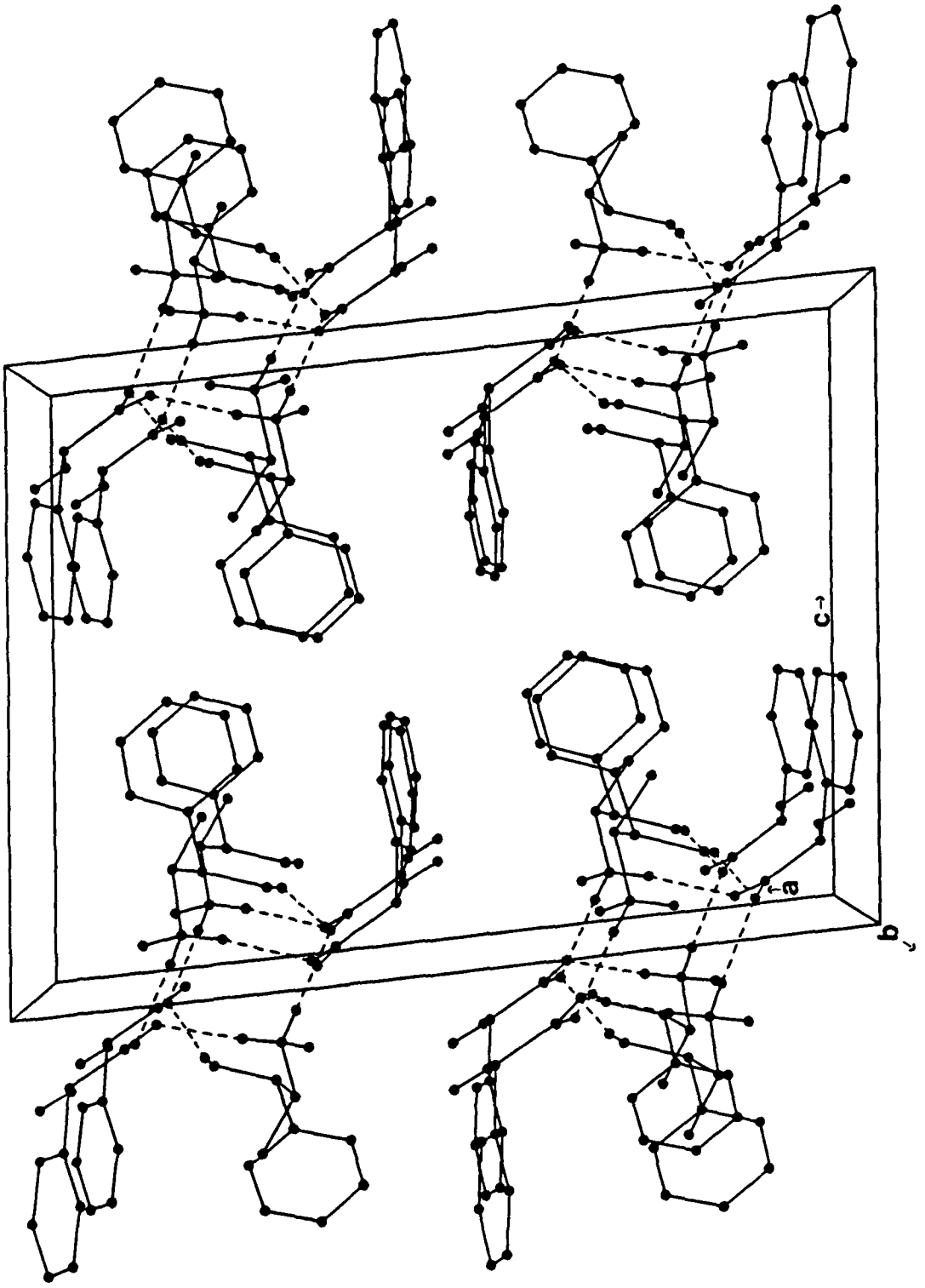

Table I. Atomic coordinates (x 10^4) of the non-H atoms in I, and their equivalent isotropic temperature factors ($Å^2$x 10^3). Esd's in parentheses.

Atom	x	y	z	U_{eq}
N(1)	1908(1)	666*	9037(1)	29(1)
O(1)	2817(1)	-2481(4)	8432(1)	43(1)
O(2)	4801(1)	409(4)	8798(1)	46(1)
O(3)	4135(1)	2646(5)	10169(1)	49(1)
O(4)	3150(1)	3281(4)	9228(1)	40(1)
C(1)	1927(1)	-3571(4)	7156(1)	29(1)
C(2)	1208(1)	-3987(5)	6832(2)	41(1)
C(3)	1072(2)	-4867(5)	5940(2)	53(1)
C(4)	1652(2)	-5366(5)	5362(2)	52(1)
C(5)	2365(2)	-4971(5)	5681(2)	48(1)
C(6)	2507(1)	-4062(5)	6570(2)	37(1)
C(7)	2063(1)	-2558(4)	8125(1)	29(1)
C(8)	1773(1)	-365(4)	8083(1)	28(1)
C(9)	2093(2)	912(5)	7291(2)	47(1)
C(10)	1363(1)	2288(5)	9249(2)	41(1)
C(11)	4300(1)	3073(4)	7752(2)	33(1)
C(12)	4200(1)	2542(5)	6785(2)	43(1)
C(13)	4367(2)	3933(7)	6070(2)	54(1)
C(14)	4634(2)	5859(6)	6309(2)	56(1)
C(15)	4727(1)	6415(6)	7267(2)	50(1)
C(16)	4559(1)	5019(5)	7982(2)	41(1)
C(17)	4152(1)	1508(4)	8528(2)	34(1)
C(18)	3793(1)	2540(4)	9384(2)	33(1)

* Coordinate fixed.

Table II. Atomic coordinates (x 10^4) of the non-H atoms in IIa, and their equivalent isotropic temperature factors ($Å^2$ x 10^3).

Atom	x	y	z	U_{eq}
N(1)	1998(2)	666*	8933(3)	57(1)
O(1)	2906(2)	-2288(14)	8466(3)	74(1)
O(2)	4538(6)	684(9)	8497(6)	198(4)
O(3)	3586(3)	4520(9)	9400(3)	99(2)
O(4)	3479(3)	1454(9)	9517(3)	90(2)
C(1)	1955(2)	-3481(9)	7175(3)	49(1)
C(2)	1228(3)	-3984(11)	6848(4)	72(2)
C(3)	1074(3)	-4906(12)	5955(4)	83(2)
C(4)	1629(4)	-5340(12)	5400(4)	80(2)
C(5)	2346(3)	-4902(10)	5716(4)	70(2)
C(6)	2516(3)	-3986(10)	6606(3)	59(2)
C(7)	2129(3)	-2370(9)	8133(3)	55(1)
C(8)	1855(3)	-364(9)	7966(3)	55(1)
C(9)	2259(5)	637(11)	7181(4)	88(2)
C(10)	1657(4)	2551(10)	8947(4)	74(2)
C(11)	4478(3)	3768(11)	7794(4)	67(2)
C(12)	4327(3)	2979(12)	6860(4)	70(2)
C(13)	4351(4)	4040(16)	6041(4)	96(3)
C(14)	4522(5)	5875(17)	6120(6)	111(4)
C(15)	4661(4)	6692(14)	7016(9)	124(4)
C(16)	4640(3)	5626(14)	7868(5)	91(3)
C(17)	4478(4)	2595(15)	8712(4)	95(3)
C(18)	3785(3)	2907(10)	9249(3)	57(2)

* Coordinate fixed.

Table III. Atomic coordinates (x 10^4) of the non-H atoms in IIb (223K structure), and their equivalent isotropic temperature factors ($Å^2$ x 10^3).

Atom	x	y	z	U_{eq}
N(1)	1998(3)	666*	8944(3)	34(1)
O(1)	2931(3)	-2263(8)	8473(3)	42(1)
O(2)	4529(4)	621(1)	8498(5)	105(2)
O(3)	3490(3)	-1465(9)	9538(3)	50(1)
O(4)	3632(3)	-4535(9)	9432(3)	55(1)
C(1)	1969(3)	-3489(9)	7175(3)	28(1)
C(2)	1230(3)	-3989(1)	6838(5)	43(2)
C(3)	1068(3)	-4919(1)	5950(5)	46(2)
C(4)	1626(4)	-5319(1)	5371(5)	43(2)
C(5)	2370(4)	-4899(1)	5701(4)	39(1)
C(6)	2535(3)	-3949(1)	6592(4)	38(1)
C(7)	2149(3)	-2349(1)	8130(4)	32(1)
C(8)	1857(4)	-359(1)	7968(4)	33(1)
C(9)	2261(5)	691(1)	7186(5)	54(2)
C(10)	1669(4)	2601(1)	8934(5)	45(2)
C(11)	4486(4)	3751(1)	7790(5)	40(1)
C(12)	4331(4)	2951(1)	6855(4)	42(1)
C(13)	4363(4)	4061(1)	6032(5)	56(2)
C(14)	4515(4)	5881(1)	6098(5)	65(2)
C(15)	4677(4)	6721(1)	7049(7)	70(2)
C(16)	4665(4)	5591(1)	7882(5)	52(2)
C(17)	4485(4)	2511(1)	8713(5)	57(2)
C(18)	3817(3)	2911(1)	9268(4)	31(1)

* Coordinate fixed.

Table IV. Atomic coordinates (x 10^4) of the non-H atoms in III, and their equivalent isotropic temperature factors ($Å^2$ x 10^3). Entries for mandelate atoms: first (2S), occupancy 0.440; second (2R), occupancy 0.560.

Atom	x	y	z	U_{eq}
N(1)	1936(2)	666*	8986(3)	58(1)
O(1)	2814(2)	-2410(9)	8450(3)	96(1)
O(2)	4714(8)	1100(18)	8708(9)	179(1)
	4813(3)	560(9)	8803(4)	60(1)
O(3)	3411(5)	4475(12)	9257(5)	70(1)
	4112(3)	2778(11)	10140(4)	69(1)
O(4)	3487(5)	1278(13)	9421(6)	79(1)
	3122(3)	3227(9)	9157(4)	59(1)
C(1)	1935(2)	-3530(7)	7159(3)	46(1)
C(2)	1214(2)	-3955(9)	6806(4)	69(1)
C(3)	1086(3)	-4850(10)	5921(5)	86(1)
C(4)	1658(3)	-5333(9)	5360(4)	74(6)
C(5)	2363(3)	-4936(9)	5702(9)	67(1)
C(6)	2503(2)	-4026(9)	6593(9)	58(1)
C(7)	2070(2)	-2460(7)	8127(3)	49(1)
C(8)	1808(3)	-354(8)	8035(3)	58(1)
C(9)	2160(5)	778(10)	7244(4)	133(1)
C(10)	1465(4)	2388(10)	9121(4)	94(1)
C(11)	4463(3)	3984(9)	7786(4)	43(1)
	4307(2)	3161(8)	7761(3)	54(1)
C(12)	4319(3)	3111(9)	6879(4)	56(1)
	4210(2)	2597(8)	6789(3)	79(1)
C(13)	4333(3)	4245(9)	6038(4)	73(1)
	4363(2)	3925(8)	6058(3)	76(1)
C(14)	4491(3)	6252(9)	6104(4)	103(1)
	4612(2)	5816(8)	6298(3)	77(1)
C(15)	4635(3)	7125(9)	7011(4)	104(1)
	4709(2)	6380(8)	7270(3)	72(1)
C(16)	4621(3)	5992(9)	7852(4)	76(1)
	4556(2)	5053(8)	8001(3)	63(1)
C(17)	4462(6)	2866(20)	8743(8)	89(1)
	4144(4)	1692(12)	8492(6)	52(1)
C(18)	3742(5)	2963(14)	9197(6)	59(1)
	3770(4)	2580(11)	9358(6)	48(1)

* Coordinate fixed.

Table V. Interionic interactions in I, IIa, IIb, and III. Entries are distances for X···O and H···O in Å; esd's ≤ 0.02, ≤ 0.05Å, respectively; and angle X-H··O in degrees, esd's ≤ 3.0°.

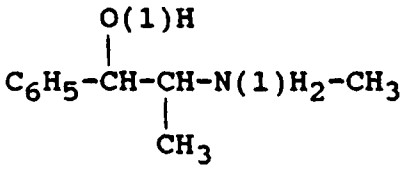

Ephedrinium Ion

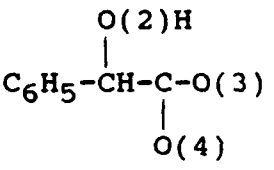

Mandelate Ion

X-H···O		Structures		
		I L-salt	IIa / IIb M-salt	III Mixed salt
X	O			
N(1)[a]	O(3)	2.80, 2.43, 124.0	2.73, 1.92, 156.1 2.71, 1.76, 156.0	3.04, 2.30, 134.8 2.67, 1.88, 141.4
N(1)[a]	O(4)	2.88, 2.05, 177.1	(3.83) (3.79)	3.06, 2.16, 161.9 (3.81)
N(1)	O(4)	2.84, 2.08, 152.0	2.75, 1.92, 168.1 2.74, 1.76, 166.0	2.77, 2.01, 143.0 2.87, 2.00, 168.5
O(1)[b]	O(4)	3.04, 2.19, 173.3		3.16, 2.32, 168.6
O(1)[b]	O(3)		2.83, 2.05, 151.2 2.84, 1.88, 179.0	2.60, 1.76, 165.4
O(2)[c]	O(3)	2.78, 1.94, 171.2		2.80, 1.96, 170.2
O(2)[c]	O(4)		(4.26) (4.13)	(4.04)
O(2)	O(3)[c]	2.78, 1.94, 171.2		2.80, 1.96, 170.2
O(2)	O(4)[c]		(4.26) (4.13)	(4.04)
O(2)[c']	O(3)			2.82, 2.10, 141.7

Notes: Distances enclosed in parentheses are between corresponding but non-interacting atoms and are included for comparison. Transformations: [a] at ½+x,½+y,2-z; [b] at x,1+y,z; [c] at 1-x,y,2-z. (') designates X,O of (2S)→(2R) mandelate interaction.

Table VI. Comparison of configuration and conformation of the ephedrinium and mandelate ions between the room-temperature structures through average of r.m.s deviations (in Å) of the non-H atoms; ephedrinium (E) = N(1), O(1), C(1)-C(10); mandelate (M) = O(2)-O(4), C(11)-C(18).

		Fitting Orthogonal Coordinates				
Structure/Moiety→		IIa		III		
↓		E	M	E	M_A	M_B
I	E	0.1148		0.0451		
	M		0.7709		0.7853	0.0380
IIa	E			0.0740		
	M				0.1367	0.7549

Table VII. Bond lengths (Å) and interbond angles (°) for the non-H atoms in the three structures. (Esd's in parentheses.)

	I	IIa	IIb	III	
				A	B
N(1)-C(8)	1.500(3)	1.503(5)	1.503(6)	1.489(6)	
N(1)-C(10)	1.486(3)	1.484(7)	1.492(8)	1.469(8)	
O(1)-C(7)	1.421(2)	1.420(6)	1.42(1)	1.396(6)	
O(2)-C(17)	1.420(3)	1.406(14)	1.382(9)	1.286(18)	1.480(9)
O(3)-C(18)	1.239(3)	1.233(10)	1.261(9)	1.196(13)	1.218(9)
O(4)-C(18)	1.275(3)	1.251(9)	1.226(7)	1.281(13)	1.270(9)
C(1)-C(2)	1.393(3)	1.381(7)	1.387(8)	1.398(6)	
C(1)-C(6)	1.392(3)	1.384(7)	1.393(8)	1.377(7)	
C(1)-C(7)	1.513(3)	1.527(7)	1.525(5)	1.527(7)	
C(2)-C(3)	1.381(4)	1.381(9)	1.374(7)	1.371(9)	
C(3)-C(4)	1.385(4)	1.352(9)	1.367(8)	1.376(9)	
C(4)-C(5)	1.379(4)	1.349(8)	1.380(9)	1.364(8)	
C(5)-C(6)	1.387(3)	1.379(7)	1.382(8)	1.384(7)	
C(7)-C(8)	1.527(3)	1.528(9)	1.522(6)	1.511(7)	
C(8)-C(9)	1.514(3)	1.533(9)	1.524(7)	1.512(9)	
C(11)-C(12)	1.394(3)	1.387(8)	1.39(1)	1.395*	1.395*
C(11)-C(16)	1.390(4)	1.364(13)	1.35(1)	1.395*	1.395*
C(11)-C(17)	1.517(3)	1.503(10)	1.531(9)	1.525(13)	1.464(10)
C(12)-C(13)	1.389(4)	1.351(10)	1.37(1)	1.395*	1.395*
C(13)-C(14)	1.385(6)	1.352(16)	1.32(1)	1.395*	1.395*
C(14)-C(15)	1.385(4)	1.348(15)	1.42(1)	1.395*	1.395*
C(15)-C(16)	1.391(4)	1.390(14)	1.392(8)	1.395*	1.395*
C(17)-C(18)	1.533(3)	1.528(8)	1.509(7)	1.489(15)	1.537(11)

Table VIII. Interbond angles (°) for the non-H atoms in the three structures. (Esd's in parentheses.)

	I	IIa	IIb	III A	III B
C(8)-N(1)-C(10)	114.0(2)	115.3(4)	114.3(4)	115.1(4)	
C(2)-C(1)-C(6)	119.1(2)	118.3(5)	118.3(5)	118.2(4)	
C(2)-C(1)-C(7)	119.6(2)	120.4(4)	120.7(4)	119.8(4)	
C(6)-C(1)-C(7)	121.3(2)	121.3(4)	120.9(4)	121.9(4)	
C(1)-C(2)-C(3)	120.4(2)	119.8(5)	120.4(5)	120.2(5)	
C(2)-C(3)-C(4)	120.2(2)	120.8(5)	120.7(5)	121.1(5)	
C(3)-C(4)-C(5)	119.6(2)	120.5(6)	120.3(5)	119.1(5)	
C(4)-C(5)-C(6)	120.7(2)	120.0(5)	119.0(5)	120.6(5)	
C(1)-C(6)-C(5)	119.9(2)	120.6(4)	121.2(6)	120.9(4)	
O(1)-C(7)-C(1)	114.0(2)	113.1(4)	113.7(9)	112.9(4)	
O(1)-C(7)-C(8)	107.8(2)	107.4(5)	108.(1)	107.3(4)	
C(1)-C(7)-C(8)	109.4(2)	109.4(4)	109.8(3)	110.2(4)	
N(1)-C(8)-C(7)	110.1(1)	108.2(3)	107.8(4)	109.7(3)	
N(1)-C(8)-C(9)	109.9(2)	109.2(5)	109.2(4)	110.5(4)	
C(7)-C(8)-C(9)	113.9(2)	112.2(12)	111.7(4)	113.3(5)	

Table VIII (continued).

	I	IIa	IIb	III	
				A	B
C(12)-C(11)-C(16)	118.8(2)	118.9(6)	120.0(6)	120*	120*
C(12)-C(11)-C(17)	119.8(2)	120.3(6)	119.4(6)	116.3(5)	122.8(4)
C(16)-C(11)-C(17)	121.4(2)	120.8(7)	120.5(6)	123.7(5)	117.2(4)
C(11)-C(12)-C(13)	120.2(3)	120.1(8)	119.1(7)	120*	120*
C(12)-C(13)-C(14)	120.5(3)	120.7(7)	122.(1)	120*	120*
C(13)-C(14)-C(15)	119.9(3)	120.8(9)	119.6(8)	120*	120*
C(14)-C(15)-C(16)	119.5(3)	119.5(10)	118.0(6)	120*	120*
C(11)-C(16)-C(15)	121.2(2)	120.0(7)	121.0(6)	120*	120*
O(2)-C(17)-C(11)	111.3(2)	111.5(6)	112.6(5)	114.3(10)	110.8(6)
O(2)-C(17)-C(18)	112.9(2)	109.0(7)	111.0(5)	112.5(11)	112.0(6)
C(11)-C(17)-C(18)	110.2(2)	112.9(6)	112.0(6)	113.2(8)	112.9(6)
O(3)-C(18)-O(4)	123.8(2)	125.8(5)	125.0(6)	124.0(10)	124.7(7)
O(3)-C(18)-C(17)	119.6(2)	118.9(6)	121.0(6)	121.9(10)	120.4(6)
O(4)-C(18)-C(17)	116.6(2)	115.2(7)	114.1(5)	113.8(9)	114.6(6)

* - Phenyl ring geometry fixed.

Table IX. Comparison of some features bearing on crystal cohesion for selected organoammonium carboxylate diastereomers. (Upper/lower entries for Less/More soluble salts.)

Cation	Anion[a]	S.G.#[b] Helical 2_1 Axis	Axial Distance (Å)	Interion H-bonds[c]	H-bond Pattern[d]	Sol'y.[e]	MP /K	Vol. /ion pr. /Å^3	Ref.[f]
PEA	2PP	19 c	5.80	3	$C_2^1(4)$	7.8	438	361	15
		4 c[g]	6.56	3	"	11.3	419	405	15
PEA	2PB	19 c	5.82	3	$C_2^1(4)$	5.6	438	402	16
		76 c	6.41	3	"	30.0	407	444	17
PEA	Man	- -	-	-	-	4.0	451	-	-
		19 b	6.87	3 (1)	$C_2^1(4)$	23.0	382	369	18
Eph	Man	5 b	6.52	3[h](3)	$C_2^1(4)$	([i])	443	411	6
		19 c	7.24	2 (2)	"		384	438	6
Eph	Man	5 b	6.54	3[h](3)	$C_2^1(4)$	6.3	443	412	this
		5 b	7.16	2 (1)	"	80.6	364	434	work
PsEph	Man	19 c	7.03	2 (1)	$C_2^2(6)$	([i])	383	442	6
		19 c	7.26	2 (1)	$C_2^1(4)$		381	437	6

[a] PEA - 1-phenylethylammonium; Eph - ephedrinium; PsEph - pseudoephedrinium; 2PP - 2-phenylpropanoate; 2PB - 2-phenylbutanoate; Man - 2-phenyl-2-hydroxyethanoate (mandelate).

[b] Space group numbers: 4 - $P2_1$; 5 - C2; 19 - $P2_12_12_1$; 76 - $P4_1$.

[c] Number in the helical chain between ammoniums and carboxylates; in parentheses the number of other interionic H-bonds, involving hydroxyls, is given if any.

[d] Helical H-bond pattern; scheme defined in ref. 14.

[e] At ambient temperature in ethanol or water, solubilities in g/100g solvent (ref. 2); melting points (ref. 2 and as cited).

[f] See References for the crystal structures.

[g] Monoclinic c axis unique; others have conventional settings.

[h] One direct and one bifurcated $R_1^2(4)$ type; 2 donor H's, 3 acceptor O's (see text).

[i] Solubilities not reported or not applicable; enthalpies of fusion suggest the likely order of solubility for these phases.